The aspect ratio effect on plasmonic properties and biosensing of bonding mode in gold elliptical nanoring arrays

Chia-Yang Tsai, Kai-Hao Chang, Che-Yao Wu, and Po-Tsung Lee*

Department of Photonic & Institute of Electro-Optical Engineering, National Chiao Tung University, Rm. 413, CPT Building, 1001 Ta-Hsueh Road, Hsinchu 30010, Taiwan

potsung@mail.NCTU.edu.tw

Abstract: We investigate both numerically and experimentally the optical properties and biosensing of gold elliptical nanoring (ENR) arrays with various aspect ratios. The gold ENR exhibits a strong localized surface plasmon bonding mode in near-infrared region, whose peak wavelength is red-shifted as increasing the aspect ratio under longitudinal and transverse polarizations. Furthermore, the disk- and hole-like optical properties for longitudinal and transverse modes are observed, which cause different behaviors in field intensity enhancement. For biomolecule sensing, we find that both modes show increased surface sensitivities when enlarging the aspect ratio of gold ENR.

OCIS codes: (240.6680) Surface plasmons; (280.4788) Optical sensing and sensors.

References and links

1. J. N. Anker, W. P. Hall, O. Lyandres, N. C. Shah, J. Zhao, and R. P. Van Duyne, "Biosensing with plasmonic nanosensors," Nat. Mater. **7**(6), 442–453 (2008).
2. K. M. Mayer and J. H. Hafner, "Localized surface plasmon resonance sensors," Chem. Rev. **111**(6), 3828–3857 (2011).
3. S. A. Maier, P. G. Kik, H. A. Atwater, S. Meltzer, E. Harel, B. E. Koel, and A. A. G. Requicha, "Local detection of electromagnetic energy transport below the diffraction limit in metal nanoparticle plasmon waveguides," Nat. Mater. **2**(4), 229–232 (2003).
4. N. Fang, H. Lee, C. Sun, and X. Zhang, "Sub-diffraction-limited optical imaging with a silver superlens," Science **308**(5721), 534–537 (2005).
5. Y. Tanaka and K. Sasaki, "Efficient optical trapping using small arrays of plasmonic nanoblock pairs," Appl. Phys. Lett. **100**(2), 021102 (2012).
6. E. Hao and G. C. Schatz, "Electromagnetic fields around silver nanoparticles and dimers," J. Chem. Phys. **120**(1), 357–366 (2004).
7. A. M. Kern and O. J. F. Martin, "Excitation and reemission of molecules near realistic plasmonic nanostructures," Nano Lett. **11**(2), 482–487 (2011).
8. G. Gantzounis, N. Stefanou, and N. Papanikolaou, "Optical properties of periodic structures of metallic nanodisks," Phys. Rev. B **77**(3), 035101 (2008).
9. M. Rang, A. C. Jones, F. Zhou, Z. Y. Li, B. J. Wiley, Y. Xia, and M. B. Raschke, "Optical near-field mapping of plasmonic nanoprisms," Nano Lett. **8**(10), 3357–3363 (2008).
10. S. Zhang, K. Bao, N. J. Halas, H. Xu, and P. Nordlander, "Substrate-induced Fano resonances of a plasmonic nanocube: a route to increased-sensitivity localized surface plasmon resonance sensors revealed," Nano Lett. **11**(4), 1657–1663 (2011).
11. M. Zhang, X. Zhou, and Y. Fu, "Plasmonic resonance excited extinction spectra of cross-shaped Ag nanoparticles," Plasmonics **5**(4), 355–361 (2010).
12. P. Y. Chung, T. H. Lin, G. Schultz, C. Batich, and P. Jiang, "Nanopyramid surface plasmon resonance sensors," Appl. Phys. Lett. **96**(26), 261108 (2010).
13. E. Prodan, C. Radloff, N. J. Halas, and P. Nordlander, "A hybridization model for the plasmon response of complex nanostructures," Science **302**(5644), 419–422 (2003).
14. J. Ye, P. Van Dorpe, L. Lagae, G. Maes, and G. Borghs, "Observation of plasmonic dipolar anti-bonding mode in silver nanoring structures," Nanotechnology **20**(46), 465203 (2009).
15. J. Aizpurua, P. Hanarp, D. S. Sutherland, M. Käll, G. W. Bryant, and F. J. García de Abajo, "Optical properties of gold nanorings," Phys. Rev. Lett. **90**(5), 057401 (2003).
16. M. B. Mohamed, V. Volkov, S. Link, and M. A. El-Sayed, "The 'lightning' gold nanorods: fluorescence enhancement of over a million compared to the gold metal," Chem. Phys. Lett. **317**(6), 517–523 (2000).

#187949 - $15.00 USD Received 29 Mar 2013; revised 16 May 2013; accepted 28 May 2013; published 5 Jun 2013

17. J. Zuloaga, E. Prodan, and P. Nordlander, "Quantum plasmonics: optical properties and tunability of metallic nanorods," ACS Nano **4**(9), 5269–5276 (2010).
18. C. Y. Tsai, S. P. Lu, J. W. Lin, and P. T. Lee, "High sensitivity plasmonic index sensor using slablike gold nanoring arrays," Appl. Phys. Lett. **98**(15), 153108 (2011).
19. H. Wei, A. Reyes-Coronado, P. Nordlander, J. Aizpurua, and H. Xu, "Multipolar plasmon resonances in individual Ag nanorice," ACS Nano **4**(5), 2649–2654 (2010).
20. A. D. Rakic, A. B. Djurišic, J. M. Elazar, and M. L. Majewski, "Optical properties of metallic films for vertical-cavity optoelectronic devices," Appl. Opt. **37**(22), 5271–5283 (1998).
21. R. A. Synowicki, "Spectroscopic ellipsometry characterization of indium tin oxide film microstructure and optical constants," Thin Solid Films **313–314**, 394–397 (1998).
22. F. Neubrech, A. Garcia-Etxarri, D. Weber, J. Bochterle, H. Shen, M. Lamy de la Chapelle, G. W. Bryant, J. Aizpurua, and A. Pucci, "Defect-induced activation of symmetry forbidden infrared resonances in individual metallic nanorods," Appl. Phys. Lett. **96**(21), 213111 (2010).
23. N. Félidj, G. Laurent, J. Aubard, G. Lévi, A. Hohenau, J. R. Krenn, and F. R. Aussenegg, "Grating-induced plasmon mode in gold nanoparticle arrays," J. Chem. Phys. **123**(22), 221103 (2005).
24. H. Wang, D. W. Brandl, F. Le, P. Nordlander, and N. J. Halas, "Nanorice: a hybrid plasmonic nanostructure," Nano Lett. **6**(4), 827–832 (2006).
25. A. G. Brolo, R. Gordon, B. Leathem, and K. L. Kavanagh, "Surface plasmon sensor based on the enhanced light transmission through arrays of nanoholes in gold films," Langmuir **20**(12), 4813–4815 (2004).

1. Introduction

Noble metal nanoparticles have unique optical properties arising from the excitation of localized surface plasmon resonance (LSPR) which produces a large local field enhancement. Such merit is currently attracting tremendous interest and important for a wide range of emerging applications, from chemical and biological sensing [1,2] to subwavelength waveguiding [3] or imaging [4] and nanoparticle trapping [5]. In particular, the ability to generate high field enhancements is determined by the geometry of the nanoparticles [6,7]. Thereby the characteristics of a myriad of nanostructures including disks [8], triangles [9], cubes [10], crosses [11], and pyramids [12] have been explored in recent years. Among various metal nanostructures, elliptical nanoring (ENR) is a hybrid nanoparticle geometry that offers the highly tunable plasmon resonances essentially arising from plasmon hybridization between an oval-shaped nanodisk and an elliptical nanohole. This hybridization results in two plasmonic modes which are the low-energy symmetric bonding mode and the high-energy asymmetric antibonding mode respectively [13,14]. Significantly, the bonding mode is beneficial to some applications since it exhibits enormous field enhancement around NR because of the symmetric charge distribution which can be regarded as a strong dipolar mode [15]. Moreover, for such elongated structure, the longitudinal plasmon resonance provides strong near-field around the two extremities due to the lightning-rod effect [16] and its intensity can be further enhanced by increasing the aspect ratio [17]. These exceptional optical properties of gold ENR are expected to be exploitable for surface-enhanced Raman scattering (SERS) and biosensing.

In this study, we report the experimental and simulation results for the plasmonic properties of bonding mode in gold ENR arrays with different aspect ratios under both longitudinal and transverse polarizations. In addition, the aspect ratio effect on electric field intensity enhancement especially for the inner and outer surfaces of gold ENR is investigated. For biosensing, compared with the transverse bonding mode, we find that the longitudinal bonding mode shows the larger wavelength shift for gold ENR with the higher aspect ratio when applied to very local changes of refractive index as induced by the presence of few molecules. These results are important for the design of nanostructure-based LSPR biosensors for detecting biological interactions, such as antibody-antigen, biotin-streptavidin, and toxin-receptor interactions.

#187949 - $15.00 USD Received 29 Mar 2013; revised 16 May 2013; accepted 28 May 2013; published 5 Jun 2013

2. Device fabrication and characterization

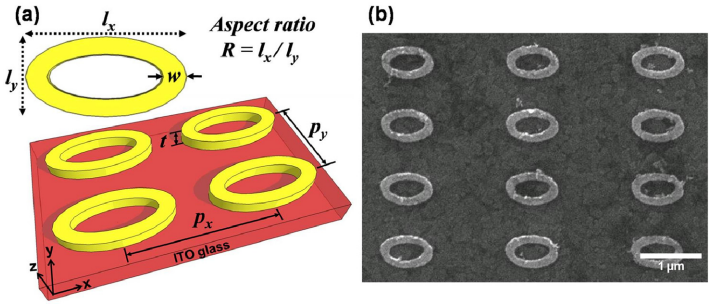

Fig. 1. (a) Geometric depiction of gold ENRs arranged in a square array on an ITO glass substrate. (b) SEM picture of a fabricated gold ENR array with w = 150 nm, l_x = 870 nm, l_y = 550 nm, t = 50 nm, p_x = 2 μm, and p_y = 1 μm.

The scheme of a square lattice gold ENR array with average ring width w, long-axis length l_x, short-axis length l_y, thickness t, periods along the long-axis direction p_x, and along the short-axis direction p_y is shown in Fig. 1(a). The aspect ratio (R) is defined as the length of long-axis l_x divided by that of short-axis l_y. In our fabrication, gold ENR arrays were manufactured on commercial indium tin oxide (ITO) glass since conducting substrate can minimize charge accumulation during electron beam lithography (EBL). First, a 150 nm polymethylmethacrylate (PMMA) layer was spin-coated onto the ITO glass. Then the ENR patterns with dimensions of 150 × 150 μm^2 and different aspect ratios were defined on the PMMA layer by EBL. After developing, the substrate was coated with a 50 nm gold thin film through thermal evaporation followed by a lift-off process. The thickness t, average ring width w, short-axis length l_y, periods p_x and p_y of fabricated gold ENR arrays are fixed at 50, 150, 550, 2000, and 1000 nm. Figure 1(b) shows a top-view scanning electron microscope (SEM) image of a fabricated gold ENR array with the aspect ratio R of 1.58.

Optical extinction measurements were performed using upright transmission spectroscopy. Collimated white light from a stabilized halogen lamp passed through a polarizer and was focused on the sample by an objective lens (NA = 0.4) at normal incidence.

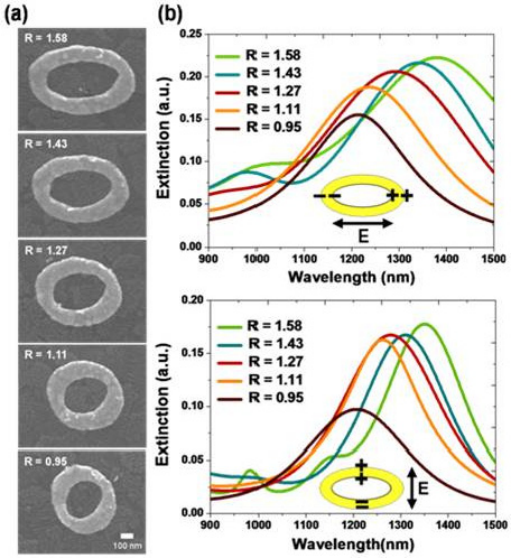

Fig. 2. (a) SEM images of gold ENRs with different aspect ratios within a range of 0.95–1.58. (b) Measured extinction spectra of gold ENR arrays with varied aspect ratio under longitudinal (top) and transverse polarizations (bottom).

#187949 - $15.00 USD Received 29 Mar 2013; revised 16 May 2013; accepted 28 May 2013; published 5 Jun 2013

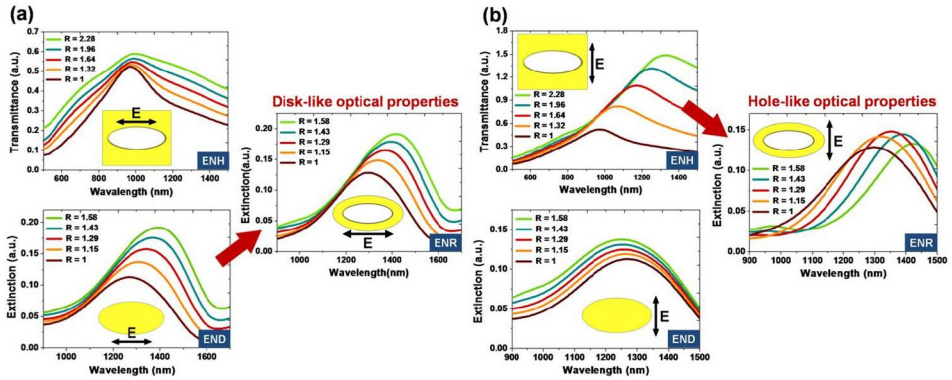

Fig. 3. Optical spectra of different nanostructures including gold ENH, END, and ENR with varied aspect ratio under (a) longitudinal and (b) transverse polarizations. Red arrows indicate that gold ENR exhibits disk- or hole-like optical properties under longitudinal or transverse polarization.

The size of focus spot is around 150 μm in diameter. The light transmitted through a gold ENR array was collected by another objective lens (NA = 0.4) into a multimode optical fiber and analyzed by an optical spectrum analyzer. To study the influence of aspect ratio on the optical behavior of gold ENR arrays, the aspect ratio is systematically varied. Figure 2(a) shows the SEM images of fabricated gold ENRs with the aspect ratios of 0.95, 1.11, 1.27, 1.43, and 1.58. Figure 2(b) shows the measured extinction spectra of gold ENR arrays with various aspect ratios under longitudinal and transverse polarizations. A resonance mode typically located at the near-infrared (NIR) spectral region can be identified as the bonding mode [18]. The charge distribution of the bonding modes show the same signs at the inner and outer surfaces of the ENR for different polarizations, shown as the insets of Fig. 2(b). As increasing the aspect ratio, the peak wavelengths of longitudinal and transverse bonding modes show apparent redshifts. Furthermore, for larger aspect ratio, the induced high-order modes under different polarizations are observed, which is in good agreement with the previous report for high-aspect-ratio plasmonic nanostructures [19].

To confirm the effect of aspect ratio on plasmonic behaviors for longitudinal and transverse polarizations, we calculated the extinction spectra of gold ENRs using 3D finite element method by COMSOL multiphysics software. Optical responses of gold elliptical nanodiscs (ENDs) and nanoholes (ENHs) with different aspect ratios were also studied since the plasmonic properties of a gold ENR can be seen as the combination of those of both nanostructures. In simulation, Lorentz-Drude model was employed to describe the dielectric function of gold [20] and we also took the dispersion of ITO film into account [21]. The simulation parameters of ENRs were chosen to be the same as those of the experimentally fabricated ones. Figures 3(a) and 3(b) show the simulated optical spectra of gold ENH, END, and ENR with different aspect ratios under longitudinal and transverse polarizations respectively. The higher order peaks observed in the measured extinction spectra are not clearly visible in the short wavelength range in the simulated spectra. This can be ascribed to the symmetry breaking by structural deviations of the nanoring from the ideal shape in experiments, which might break the symmetry of the collective charge oscillation and lead to the excitation of higher order modes [22]. In addition, the simulated peaks are located at longer wavelengths when compared with the measured ones. This is because the simulated extinction spectra were calculated for a single gold ENR. However, ENR arrays were used in our experiments. The restoring force of gold ENR would be strengthened for periodic array due to the in-phase addition of radiation fields (far-field coupling), which leads to the shifts of LSPR peaks toward shorter wavelengths [23]. The peak wavelengths of bonding mode in gold ENR show obvious redshifts with increasing the aspect ratio under both polarizations. It is clear that the computational results for both modes are in good agreement with the experimentally observed trends. Under longitudinal polarization, large redshift can also be

#187949 - $15.00 USD Received 29 Mar 2013; revised 16 May 2013; accepted 28 May 2013; published 5 Jun 2013

found from the dipole mode in gold END, as shown in Fig. 3(a). This means that the characteristic of bonding mode in gold ENR is mainly contributed from nanodisk plasmons for longitudinal polarization. Under transverse polarization, the bonding mode in gold ENR exhibits a redshift similar to the behavior of the cavity mode in gold ENH with increasing the aspect ratio, as shown in Fig. 3(b). Therefore, we can understand that the characteristic of bonding mode in gold ENR is mainly contributed from nanohole plasmons for transverse polarization. These results indicate that gold ENR shows the disc- or hole-like plasmonic properties under longitudinal or transverse polarization. These properties can be understood from plasmon hybridization, which have also been explored in the previous work for metal nanorice [24].

Furthermore, near-field intensity enhancement profiles of the bonding mode in gold ENR with the largest aspect ratio (R = 1.58) under longitudinal and transverse polarizations were simulated, as shown in Fig. 4(a). The intensity enhancement is defined as the ratio of near-field intensity of gold ENR to incident field intensity. Clearly the field intensity enhancement is very dissimilar under different polarizations. The high-aspect-ratio gold ENR produces an apparent intensity enhancement located at the outer surface under longitudinal polarization, while under transverse polarization the larger intensity enhancement near the inner surface of gold ENR is observed. In addition, for such hollow nanostructure, we calculated intensity enhancements at the inner and outer surfaces of gold ENR with varied aspect ratio, as shown in Fig. 4(b). The inset shows the two point monitors at the inner (P_{inner}) and outer (P_{outer}) surfaces of gold ENR used to calculate the intensity enhancement. Under longitudinal polarization, the intensity enhancement at the outer surface of gold ENR is raised as the aspect ratio is increased. However, the decreased enhancement with increasing the aspect ratio for the inner surface of gold ENR is obtained. Significantly, the trend is reversed under transverse polarization. All of these observations can be understood from the nature of the bonding mode in gold ENR. Under longitudinal polarization, the bonding mode is dominated by the disk-like mode, which results in the larger field intensity enhancement at the outer surface of ENR compared with that at the inner surface. Oppositely, the transverse bonding mode in gold ENR with high aspect ratio shows larger enhancement of field intensity at the inner ENR surface resulting from the dominated hole-like mode. This further elucidates that the trends in optical spectra for the longitudinal and transverse bonding modes are dominated by the disk and hole plasmon modes respectively. Moreover, for the transverse bonding mode, the

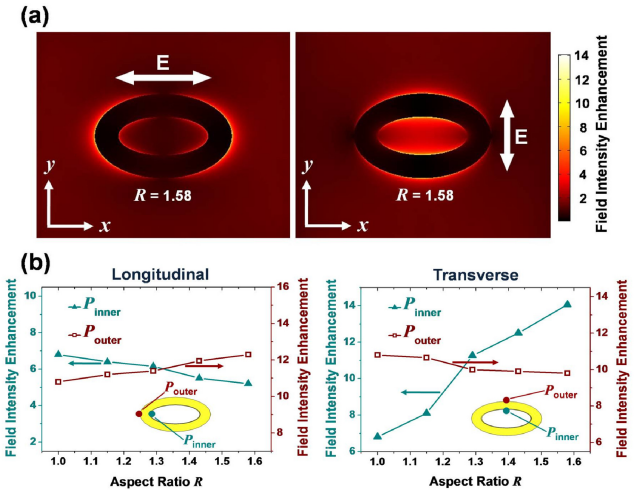

Fig. 4. (a) Near-field intensity enhancement mapped on the top surface of gold ENR with the aspect ratio of 1.58 under longitudinal (left) and transverse (right) polarizations. (b) The field intensity enhancement at the inner and outer surfaces (denoted by the P_{inner} and P_{outer}) of gold ENR as a function of aspect ratio under different polarizations.

#187949 - $15.00 USD Received 29 Mar 2013; revised 16 May 2013; accepted 28 May 2013; published 5 Jun 2013

intensity enhancement at the inner surface is dramatically increased as enlarging the aspect ratio. Since an incident electric field separates positive and negative charges in metal along the short axis of ENR and gold ENR shows hole-like plasmonic properties under transverse polarization, the number of induced charge dipoles and the resulting dipole moments at the inner surface would grow considerably due to the significant extending of inner surface area as we increase the aspect ratio. Thus, we speculate that the large intensity enhancement arises from the greatly increased amount of charge dipoles on the inner surface of ENR.

3. Biosensing properties

For biosensing, the gold ENR arrays were applied to detect the binding of protein (bovine serum albumin, BSA). Figure 5(a) shows the illustration of BSA binding process. First, to improve the immobilization efficiency of BSA capture on the samples, the gold ENR surfaces were modified with a self-assembled monolayer (SAM) of mercaptoundecanoic acid (MUA) for 24 hours. Subsequently, activation of the acid of MUA was performed by immersing the samples in a solution of 1-ethyl-3-(3-dimethylaminopropyl) carbodiimide (75mM) and N-hydroxysuccinimide (15 mM) in 0.1 M phosphate buffer saline (PBS) for 30 minutes. The samples with activated MUA surfaces were then incubated in a solution of BSA (5 g/L in PBS, pH 7.4) for 1 hour. After each step of the binding process, the samples were blown dry by a stream of nitrogen gas and optically characterized. Figure 5(b) shows normalized extinction spectra of longitudinal bonding mode in gold ENR array with the aspect ratio R of 1.58 before and after modification with MUA and after BSA binding. Apparently, after surface modification of gold ENRs, there is a 13 nm redshift (from 1370 to 1383 nm) for the longitudinal bonding mode. An additional redshift of 22 nm (from 1383 to 1405 nm) is observed when BSA is bound to the MUA. The total LSPR shift of 35 nm of gold ENR array for binding of BSA to a MUA-coated gold surface is larger than that from the previous work using gold nanohole array under the similar BSA concentration [25]. This high surface sensitivity demonstrates that gold ENR array has the potential to probe a nanoscale region around the ENR particle for observing molecular interactions. Figure 5(c) shows the LSPR shifts of bonding mode in gold ENR array with varied aspect ratio under different polarizations. We find that both longitudinal and transverse bonding modes show increased surface sensitivities as enlarging the aspect ratio mainly resulting from the expansion of sensing area. Moreover, as the aspect ratio is enlarged, the sensitivity of the longitudinal

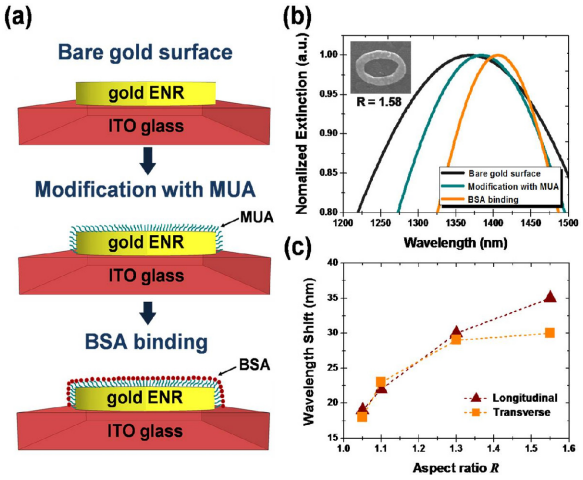

Fig. 5. (a) Illustration of experimental procedure for biosensing including surface modification of gold ENR and BSA protein binding. (b) Normalized extinction spectra of longitudinal bonding mode in gold ENR array with R = 1.58 for each step of biosensing experiment. (c) Total LSPR wavelength shifts of longitudinal and transverse bonding modes induced by MUA modification and BSA binding as a function of aspect ratio of gold ENR.

#187949 - $15.00 USD Received 29 Mar 2013; revised 16 May 2013; accepted 28 May 2013; published 5 Jun 2013

bonding mode increases more than that of the transverse bonding mode. This is primarily because the sensing area of the disk-like mode extends more at the outer surface for the longitudinal bonding mode.

4. Summary

In summary, we studied the optical behavior and biosensing of gold ENR arrays with different aspect ratios. For the plasmonic properties, the bonding mode in gold ENR array shows apparent redshifts as increasing the aspect ratio under both polarizations. Furthermore, the disc- and hole-like optical properties of gold ENR for longitudinal and transverse polarizations are found, which exhibit stronger field intensity enhancements at the outer and inner gold ENR surfaces respectively. For biosensing performance of BSA binding, the surface sensitivity of bonding mode as a function of aspect ratio is investigated. The peak wavelength shifts of longitudinal and transverse bonding modes increase when enlarging the aspect ratio and we observe the maximum total wavelength shift of 35 nm of longitudinal bonding mode in gold ENR array with R = 1.58. This high surface sensitivity suggests that gold ENRs can serve as potential ultrasensitive biosensing elements for probing molecular interactions.

Acknowledgments

This work is supported by Taiwan's National Science Council (NSC) under Contract Nos. NSC-101-2221-E-009-054-MY2 and NSC-100-2221-E-009-109-MY3. The authors would like to thank the help from Center for Nano Science and Technology (CNST) at National Chiao Tung University (NCTU), Taiwan.